EXPERIMENTAL STUDY OF FLUID FLOW AND HEAT TRANSFER AROUND A PAIR OF CIRCULAR CYLINDERS IN STAGGERED ARRANGEMENT

A.M.E. Abd El-Latif, R.M. EL-Taher and I.A. Gad

Department of Mechanical Power Engineering, Zagazig University, Zagazig, Egypt.

ABSTRACT

Fluid flow and heat transfer around two circular cylinders in staggered arrangement subjected to a uniform free stream have been investigated experimentally. The longitudinal spacing ratio L/D was varied in the range 1-5 (L is the streamwise spacing between the cylinders centers, D is the cylinder diameter). The transverse spacing T/D was varied in the range 0-3 (T is the transverse spacing between the cylinders centers). Experiments were carried out at Reynolds number 5.8×10^4 based on cylinder diameter. Distributions of static pressure coefficient and local Nusselt number on the surface of the downstream cylinder have been determined. Two bistable flow modes were observed at L/D=3.2, and T/D=0.2 during both pressure and temperature measurements. The mean Nusselt number Nu_m is discussed in relation to T/D, and L/D. Correlations between Nu_m, T/D and L/D are obtained.

Keywords: Fluid flow, Heat transfer, Circular cylinders, Staggered arrangement

INTRODUCTION

The study of flow around two circular cylinders placed in a stream is of fundamental importance in fluid dynamics. Practical applications of this configuration are seen in various areas of engineering: heat exchangers, twin conductor transmission lines, twin chimney stacks, and off-shore structures can be mentioned among others.

Numerous efforts have been devoted to clarify the complex character of this flow configuration. Zdravkovich [1] has reviewed investigation in this area up to 1977. Subsequent to this review, some works [2-4] has been done on the same problem. These works have shown that the interference effects between the cylinders depend on their spacing and the angle between the plane of their axes and the flow direction. It was found that with some critical arrangements, the flow pattern around the cylinders changes intermittently between two types. These two types of the flow pattern induce different forces and both intermittently change over. The three-dimensional case of two cylinders of finite height subjected to a uniform flow was investigated by Zdravkovich [5]. Taniguchi *et al.* [6] measured the circumferential pressure distributions around two cylinders of finite height, vertically immersed in a turbulent boundary layer. Sayers [7] experimentally investigated flow interference between three equispaced cylinders when subjected to a cross flow. Zdravkovich [8] has made an attempt to categorize various cluster arrangements of circular cylinders in terms of the number of cylinders, their mutual spacing and orientation to the oncoming flow. Barnes *et al.* [9] investigated the flow past two cylinders having different diameters. Price and Paidoussis [10] investigated the aerodynamic forces acting on groups of two and three circular cylinders when subjected to a cross flow.

The interference effect of a wall on the flow around two circular cylinders arranged in tandem was investigated by El-Taher *et al.*[11].

The flow around two circular cylinders arranged perpendicular to each other was investigated by several authors [12-17].

The study of shear flow about two cylinders has received little attention compared to the case of uniform flow. A numerical study of the interference between two circular cylinders normal to a uniform shear flow was investigated by El-Taher [18]. Numerical results showed that interference effects in shear flow are larger than the corresponding effects in potential flow. El-Taher [19] investigated the same problem experimentally in the subcritical Reynolds number range. It was found that the free-stream shear has a stabilizing effect on the intermittent changeover of the flow patterns at the critical arrangement. EL- Taher [20] investigated the flow around two parallel circular cylinders when the flow is sheared in the axial direction of the cylinders. He studied the effect of mutual interference on pressure distributions, force distribution and vortex shedding frequency along the span of each cylinder. Kostic, and Oka [21] experimentally investigated the flow and heat transfer around two cylinders in tandem arrangement in the Reynolds number range $1.2x10^4$ <Re<$4x10^4$ and the distance between the cylinders in the interval 1.6<L/D<9.0. They found that the mean Nusselt number for the 1 st cylinder is proportional to $Re^{0.6}$, as for the single cylinder for all distances. The mean Nusselt number for the 2 nd cylinder is proportional to $Re^{0.6}$ for L>2.7D, and to $Re^{2/3}$ for L/D<2.7.

Aiba [22] investigated the heat transfer around a tube in in-line tube banks near a plane wall. Variations in the characteristic features of local and mean Nusselt number Nu_m are discussed in relation to C/D, L/D, and Re (where C is the clearance between the cylinders and the wall). The heat transfer around a pair of circular cylinders arranged side by side and normal to a stream was investigated by Sayed [23]. Variation in the characteristic features of local and mean Nusselt number are discussed in relation to H/D and Re (where H is the center line spacing).

It is seen from the previous survey that there is no work dealing with the case of convective heat transfer around two circular cylinders in staggered arrangement. The objective of the present study is to investigate the fluid flow and heat transfer characteristics around two cylinders in staggered arrangement in a uniform free stream, in subcritical Reynolds number range.

EXPERIMENTAL APPARATUS

The experiments were performed in an open type wind tunnel which has a test section of 150 mm height, 600 mm width and 1500 mm length with maximum air speed of 22.5 m/s. Figure 1 shows the general arrangement of the wind tunnel. Two smoothly machined steel cylinders of 37.5 mm outer diameter, 1.5 mm wall thickness spanned the tunnel test section vertically, thus having a length- to- diameter ratio of 4. One of the cylinders was fitted with a pressure tapping 0.5 mm in diameter at the mid-span position. The longitudinal spacing between the cylinders (L) was varied in the range 1D-5D, and the transverse spacing between the cylinders centers (T) was varied in the range 0-3D (see Figure 2). Experiments were carried out at Re = 5.8 x 10^4 based on the cylinder diameter. To adjust the spacings between the cylinders, a standard blocks with different thickness were used. Static pressure on the cylinders surface was measured by using a micromanometer with an accuracy of ± 0.01 mm of the fluid manometer.

One of the two cylinders has been constructed for heat transfer measurement (see Figure 3). The electric heater-4 made of kanthal wire, uniformly installed in ceramic core, was placed inside the cylinders. Surface temperatures were measured in the symmetry plane of the cylinder with an accuracy less than 0.01 mv using Cu-Ko thermocouples-2.

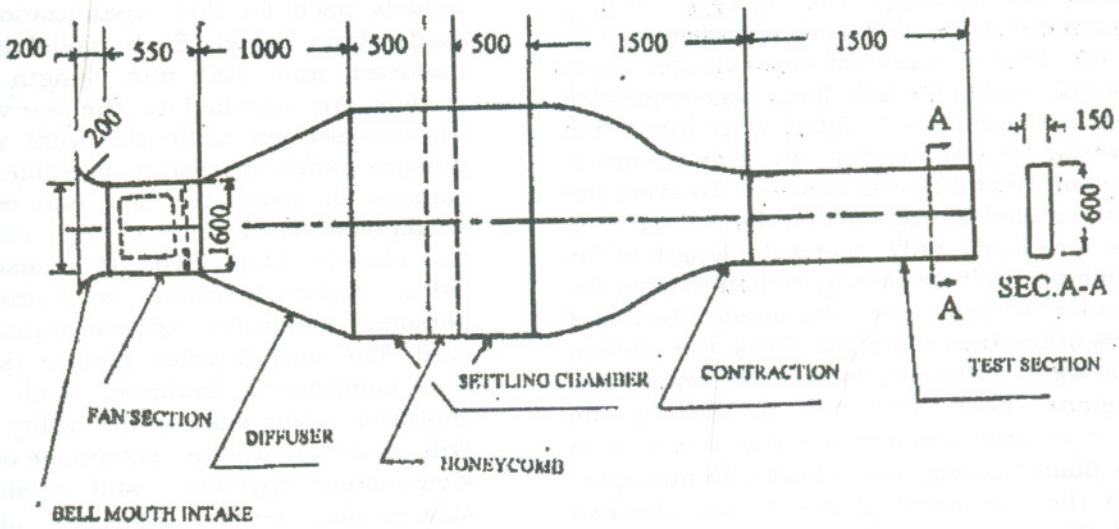

Figure 1 Wind tunnel arrangemenmt

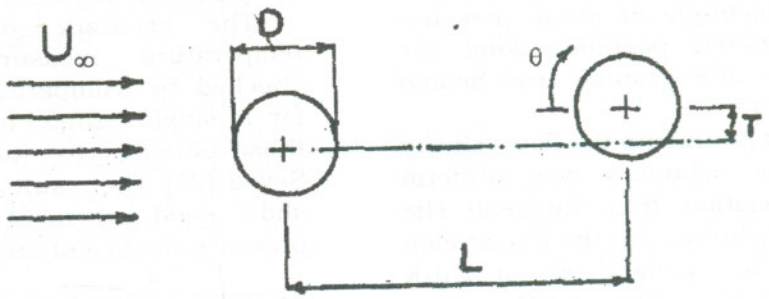

Figure 2 Sketch of staggered arrangement

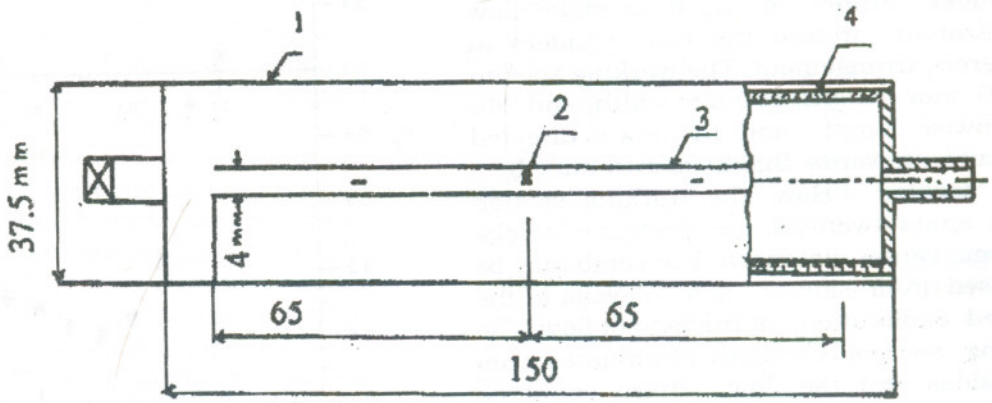

1- Cylinder wall **2- Thermocouple**
3- Groove **4- Eletric heater**

Figure 3 Temperature measuring cylinder

In order to avoid the circumferential heat conduction through the cylinder wall, a segment 4 mm wide (corresponding to 8.7° of the central angle of the cylinder cross section) and 130 mm long was separated with two grooves-3, filled with insulation material (epoxy resin). In this manner, constant heat flux was ensured. To avoid the error caused by end effects, the voltage drop was measured only along the length of the segment. The heat loss by radiation from the cylinder surface was estimated to be about 0.6% of the heat supplied. Thus, the present data were obtained under the condition of constant heat flux. By measuring the pressure and temperature distributions in two planes along the cylinder 35 mm apart from the symmetry plane, it was checked that there was no influence of side walls on the measurements in the symmetry plane. By rotating the cylinders it was possible to place the thermocouple or static pressure tap in any desired position along the perimeter. Only one cylinder was heated during experiments.

During the experiments the flow velocity upstream of the cylinders was uniform within ± 1% deviation from the mean. The temperature distribution in the free stream was surveyed by means of a Cu-K thermocouples with an accuracy less than 0.01 mv. The free stream temperature distribution was found uniform within 1.5% deviation from the mean.

Smoke tunnel is used to make flow visualization around the two cylinders in staggered arrangement. The working section is 180 mm height, 100 mm width, and 240 streamwise length, and the flow is directed vertically upwards. Smoke is introduce by a comb located below the working section which emits twenty-three streams of smoke at 7 mm center distances. The comb may be traversed from side to side to assist in the detailed exploration of the field of flow. The working section is brightly illuminated from both sides and the flow pattern could be clearly visible. The air flow velocity in the working section may be varied from zero to about 3 m/s. The two circular cylinder models used for flow visualization test are made from wood. Each model is 13 mm diameter and 100 mm length. Cylinder models are attached to the rear wall of the working section while the front wall is of prespex and is readily movable. A video camera is used to view and record the smoke-visualized flow pattern around the two models. The video tap is inserted into video system, which is connected to personal computer system through video card. The output video picture is seen on the computer's monitor, and then is captured using oak capture utility program. This system's unique advantage of variable slow-motion-playback, still framing, and slow-motion reverse playback allowed a detailed and clear picture of the flow pattern. The capture flow pattern pictures are printed using laser jet printer.

The accuracy of the pressure and temperature measurements have been checked by comparing the results obtained for a single cylinder in uniform stream with those obtained by Kostic and Oka [21] and Sayed [23]. The results displayed in Figure 4 show good agreement for the distribution of pressure coefficient and Nusselt number.

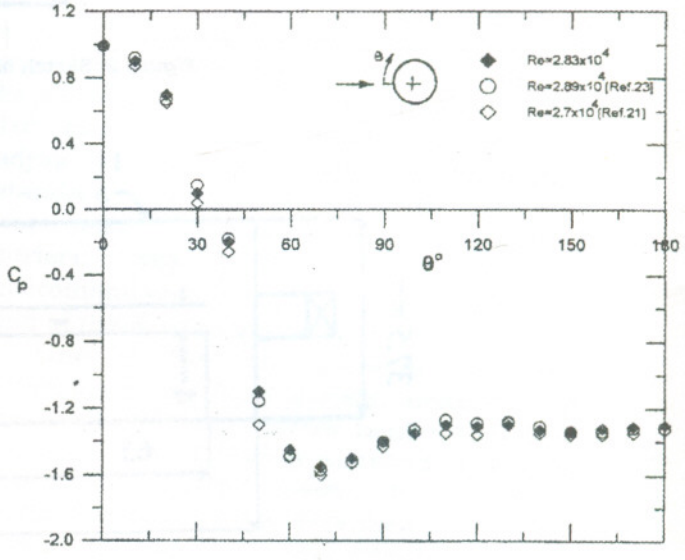

Figure 4-a Pressure distribution for a single cyliner

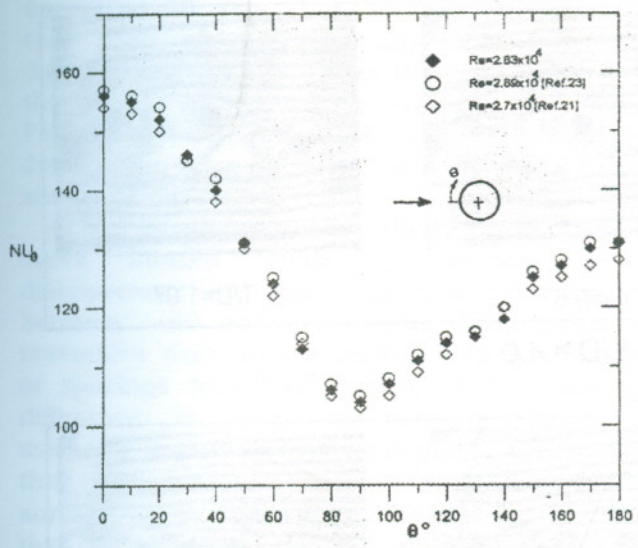

Figure 4-b Distribution of local Nusselt number for a single cylinder

EXPERIMENTAL RESULTS AND DISCUSSION

All measurements were taken at a Reynolds number of 5.8×10^4 based on the cylinder diameter and the mean velocity at the tunnel test section. The longitudinal spacing ratio (L/D) was varied in the range 1.0-5.0, and the transverse spacing ratio (T/D) was varied in the range 0.0-3.0.

Pressure Measurements

The pressure distribution around the downstream cylinder was measured at angular intervals of 5° for various staggered arrangements. Figure 5 shows the effect of transverse spacing T/D on pressure distribution around the downstream cylinder at L/D=4.0. The figure shows that at T/D> 0.0 a shift in the stagnation point was always in the direction away from the side of the upstream cylinder wake (see the flow visualization in Figure 6 for L/D=4.0 at T/D=0.53, and 1.07). Also Figure 5 shows that at the inner side of the cylinder ($-40° < \theta < -120°$) the values of C_p decreases as T/D increases. This is attributed to the increase of the flow rate in the gap between the cylinders as T/D increases, and hence the flow velocity increases and the pressure decreases. Figure 5 also shows that the pressure coefficient on the outer side of the cylinder ($40° < \theta < 140°$) is greater than that on the inner side ($-40° < \theta < -120°$), consequently the downstream cylinder has a negative lift force (force towards the axis of the upstream cylinder).

It is seen that at T/D=0.0 the shear layers separated from the upstream cylinder do not attach to the downstream one, and there is a single stagnation point at θ =0.0. The flow visualization in Figure 6 shows that (for L/D=4.0, and T/D=0.0) the flow separated from the upstream cylinder do not attach to the downstream one, and vortex streets are formed behind both cylinders.

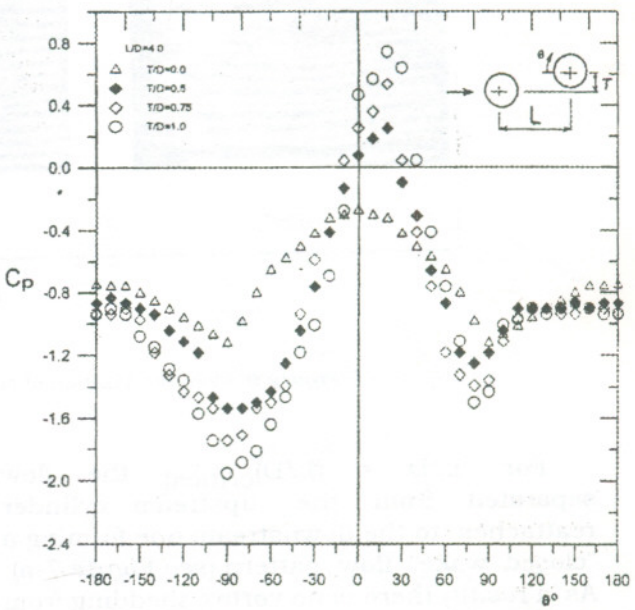

Figure 5 Effect of transverse spacing T/D on pressure distribution around the downstream cylinder at L/D=4.0 (Re = 5.8×10^4)

The results of previous measurements for two cylinders in tandem arrangement (T/D=0) described by Zdravkovich [1] have shown that at a certain critical spacing $(L/D)_{critical}$, there is an abrupt change from one stable flow pattern to another. The value of $(L/D)_{critical}$ in uniform flow ranges between 3.5 and 3.8 depending on the Reynolds number and the flow condition in the various experiments [1].

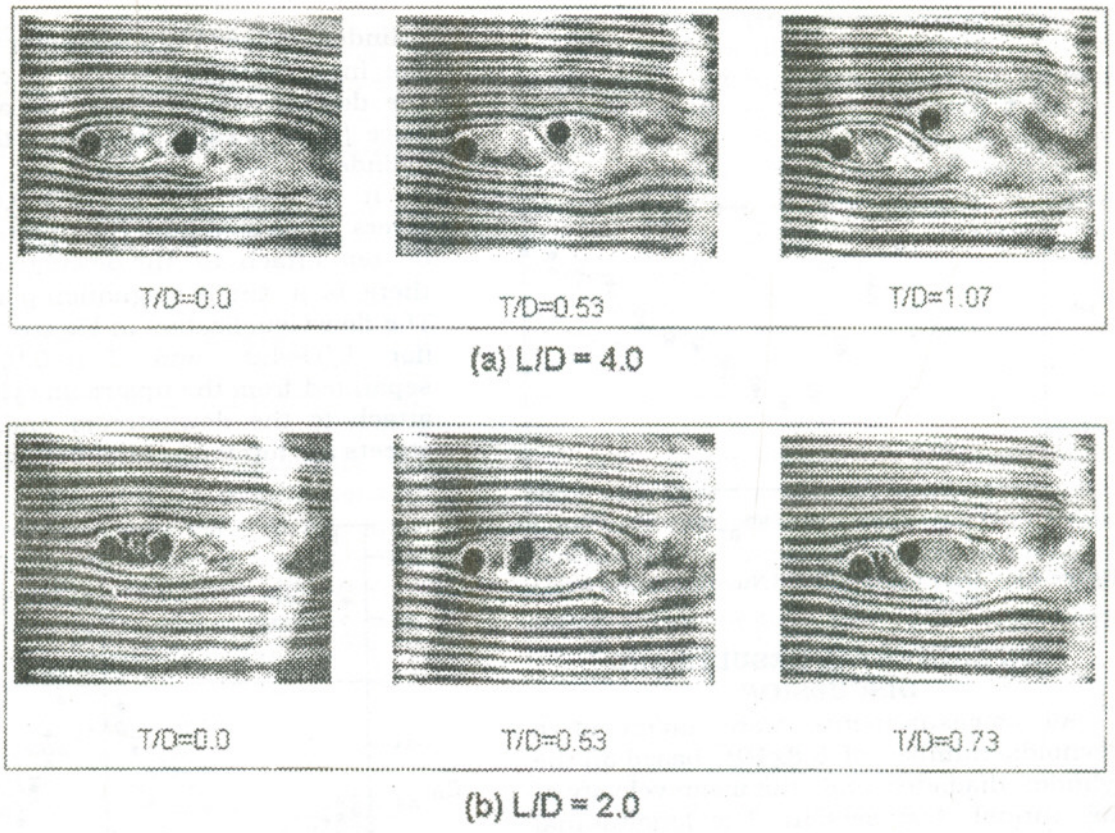

Figure 6 Flow visyalization of staggered arrangement atL/D = 2.0 and 4.0

For $L/D < (L/D)_{critical}$ the flow separated from the upstream cylinder reattaches to the downstream one forming a "closed wake" flow pattern (see Figure 7-a). As a result, there is no vortex shedding from the first cylinder. For values of $L/D > (L/D)_{critical}$, the flow separated from the upstream cylinder do not attach to the downstream one, and vortex streets are formed behind both cylinders (see Figure 7-b). In side-by-side arrangement (L/D=0, T/D > 1), it was observed by other investigators [1] that for a uniform oncoming stream, the flow about cylinders for $1.1 < \frac{T}{D} < 2.0$ is asymmetric and the flow through the gap was not stable but changed sides at irregular intervals of time. Therefore, two alternative values of lift forces, coupled with two alternative values of drag forces, are induced on each cylinder. The wakes behind the two cylinders are different due to the biased flow in the gap. One cylinder is subjected to a narrow wake and the other to a wide wake and vice versa after each change over (see Figure 8).

In the present work also a bistable flow pattern is observed at spacing L/D=3.2, and T/D=0.2. Figure 9 shows the distribution of local static pressure coefficient around the downstream cylinder at L/D=3.2, and T/D=0.2 for $Re=5.8x10^4$. Two different pressure distributions were found as shown in figure. One of the distributions (the curve labeled mode 1) has a very low pressure between -90 and -180 deg which is due to a high velocity around that side of the downstream cylinder. The stagnation point, seen as the positive pressure peak was at 45 deg, and the very low pressure did not

appear at 90 deg. These facts indicate that the bulk of the flow approaching the downstream cylinder was directed toward the gap between the cylinders (see Figure10-a). The result of such a pressure distribution was a very high lift force as shown below.

The second pressure distribution (the curve labeled mode 2) shows the disapperance of the very low pressure between -90 and -180°. The distribution resembles that for the tandem arrangement at spacings less than crictical [1]. The main difference is that the present one is markedly asymmetric. This is due to the fact that the shear layer separted from the upper surface of the upstream cylinder reattach to the downstream cylinder, while the shear layer separated from the lower surface of the upstream cylinder do not attach to the downstream one (see Figure 10-b). The result is a very small lift as shown below.

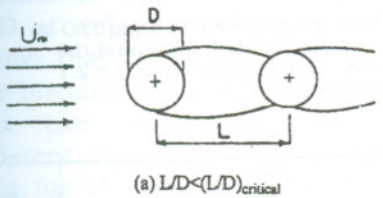

(a) $L/D<(L/D)_{critical}$

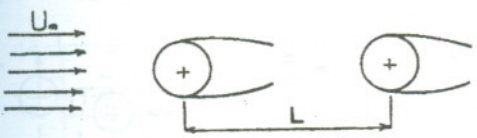

(b) $L/D>(L/D)_{critical}$

Figure 7 Schemetic illustration of flow pattern around cylinders in tandem arrangement

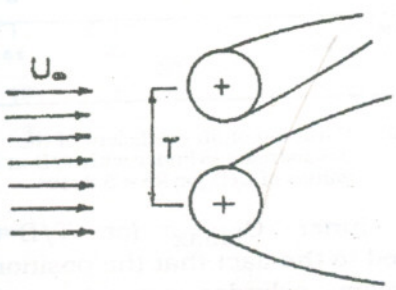

Figure 8 Schematic illustration of asymmetric wake structure behind two cylinders in the bistable flow (side-by-sid arranmement)

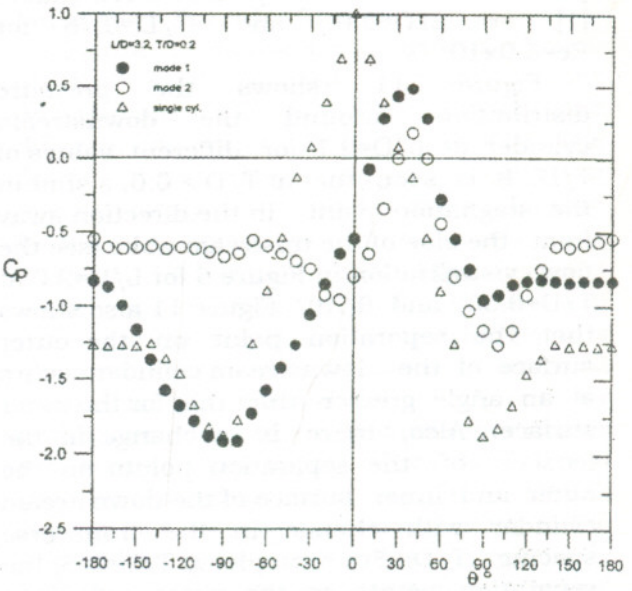

Figure 9 Pressure distribution around the downstream cylinder at L/D = 3.2, T/D = 0.2 for Re = $5.8x10^4$

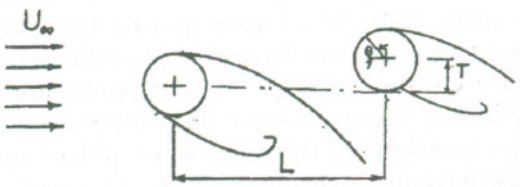

(a) Mode 1

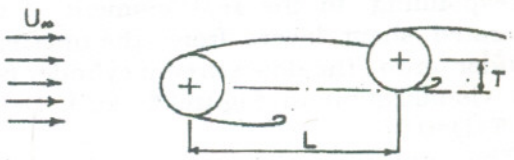

(b) Mode 2

Figure 10 Schematic illustration of the bistable flow pattern around cylinders in staggered arrangement at L/D = 3.2 and T/D = 0.2

The most striking feature of the two pressure distributions was that they changed over intermittently at irregular time intervals. This indicated a bistable flow through the gap between the cylinders at theses spacings. A similar bistable flow

pattern was observed by other investigators [1] at L/D=3.0, and T/D=0.25 for Re=6.0x10⁴.

Figure 11 shows the pressure distribution around the downstream cylinder at L/D=2.1 for different values of T/D. It is seen that at T/D > 0.0, a shift in the stagnation point in the direction away from the side of the upstream wake (see the flow visualization in Figure 6 for L/D=2.0 at T/D=0.53, and 0.73). Figure 11 also shows that the separation point on the outer surface of the downstream cylinder occurs at an angle greater than that for the inner surface. Also, there is a change in the location of the separation points on the outer and inner surface of the downstream cylinder with change in the transverse spacing (T/D). For example, at T/D=0.5, the separation points on the outer and inner surface of the downstream cylinder occur at θ=90° and -70° respectively, while at T/D=0.75 the separation points occur at θ=100°, and -80°. Consequently the width of the wake of the downstream cylinder differ with change of T/D. Flow visualization for L/D=2.0 Figure 6 also shows the change in the location of the separation points on the downstream cylinder at T/D=0.53,and 0.73. Figure 6 also shows that the wake width at T/D=0.53 is greater than that for T/D=0.73. Figure 11 shows that at T/D=0.0 there are two pressure peaks at θ=45° and -45° corresponding to the reattachment of the separated shear layers from the upstream cylinder onto the downstream cylinder (see flow visualization in Figure 6 for L/D=2.0 and T/D=0.0).

The pressure distribution about the cylinder was integrated to give the lift, and drag coefficients. Figure 12 shows variation of lift coefficient with T/D at different values of L/D. It is seen from the figure that at L/D=3.2 and T/D=0.2 there are two values for the lift coefficient. These two values corresspond to the two bistable flow modes at these values of L/D and T/D. Figure 12 also shows two peaks of lift coefficient at L/D=3.2, one at T/D=0.2, and the second at T/D=1.0. The first peak indicating the inner C_{Lmax}, and the second indicating the outer C_{Lmax}, and the magnitude of the inner C_{Lmax} is higher than the outer C_{Lmax}.

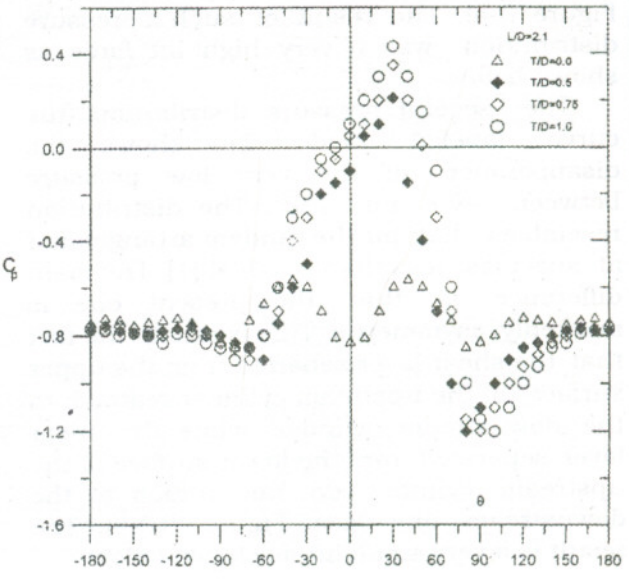

Figure 11 Effect of transverse spacing T/D on pressure distribution around the ownstream cylinder at L/D = 2.1 (Re=5.8x10⁴)

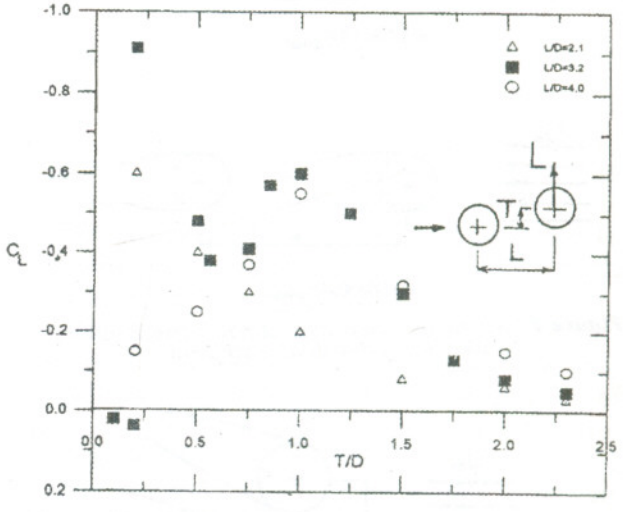

Figure 12 Variation of lift coefficient of the downstream cylinder with T/D at different values of L/D for Re = 5.8x10⁴

The inner C_{Lmax} (at T/D=0.2) is attributed to the fact that the position of the downstream cylinder suggests an intense gap flow between the two cylinders. Further reduction of the transverse spacing

(T/D<0.2) might block the gap flow with the corresponding sharp fall of the lift coefficient. The outer C_{Lmax} (at T/D=1.0) is attributed to displacement of the upstream cylinder wake by the downstream cylinder and in doing so squeezes the streamlines between its inner side and the displaced wake. At L/D=3.2, and T/D>1.0, the lift coefficient decreases gradually with T/D, this is due to the decrease of the flow rate between the inner side of the downstream cylinder and the formed wake of the upstream cylinder as T/D increases. Figure 12 shows that at L/D=2.1 the lift coefficient decreases gradually as T/D increases. For L/D=4.0 the lift coefficient increases with increasing value of T/D. C_L reaches a maximum at T/D=1.0 before it decreases back to the zero value of the isolated cylinder.

Figure 13 shows variation of drag coefficient of the downstream cylinder with T/D at different values of L/D. The figure shows that for L/D=3.2 and T/D=0.2, where the bistable flow occurs, the drag coefficient has two values, corresponding to two different pressure distributions. It is seen that for all values of L/D (2.1, 3.2, and 4.0) the drag coefficient increases regularly and gradually with the transverse spacing.

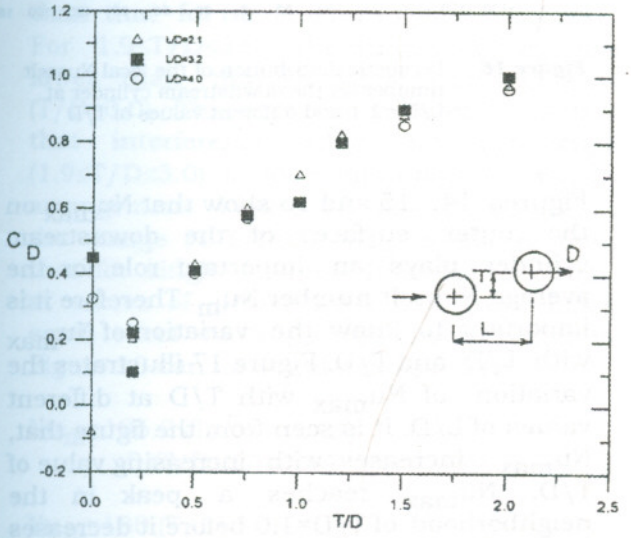

Figure 13 Variation of drag coefficient of the downstream cylinder with T/D at different values of L/D for Re = 5.8x10⁴

Local Heat Transfer Characteristics

Figure 14 shows perimetric distribution of the local Nusselt number on the downstream cylinder at L/D=4.0 and different values of T/D for Re=5.8 x10⁴. The figure shows that $Nu_{max.}$ occurs at approximately $\theta=30^{o}$, this is due to the shift in the stagnation point was always in the direction away from the side of the upstream wake (as seen in Figure 5). The symmetry of $Nu\theta$ curves about the stagnation point is also remarkable. Also it is seen that for all values of T/D, the values of Nu_θ at outer and inner sides of the downstream cylinder are greater than these values for T/D=0.0 and for a single cylinder. At T/D=0.0, Nu_{max} occurs at $\theta=0.0$ corresponding to the stagnation point, as shown in Figure 5. Figure 14 also shows that at the outer and inner surface of the downstream cylinder there are two minima at $\theta=$ 90° and 150°corresponding to the laminar boundary layer transition point, and the turbulent boundary layer separation point respectively.

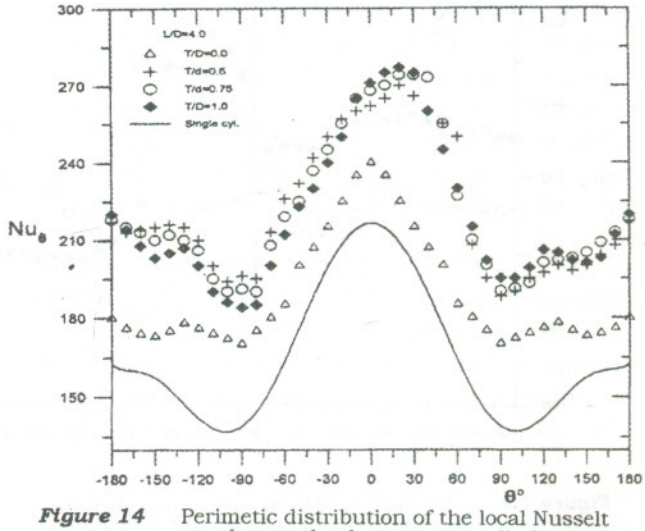

Figure 14 Perimetic distribution of the local Nusselt number on the downstream cylinder at L/D =4.0 and different values of T/D

During measurements, two bistable modes were easily observed from pressure results at L/D=3.2, and T/D=0.2. At this spacing, it was observed that surface temperature oscillated between two steady values. It was observed that the durations of

these two steady values are smaller than the corresponding durations in pressure measurements. This is attributed to the thermal time lag due to the heat capacity of the cylinder material.

Distribution of local Nusselt number Nu_θ around the downstream cylinder for L/D=3.2, and T/D=0.2 are presented in Figure 15, including the results for a single cylinder. Figure 15 shows that for mode 1, Nu_θ on the inner surface of the downstream cylinder is higher than that on the outer surface. This is attributed to the bulk of the flow approaching the downstream cylinder was directed toward the gap between the cylinders as mentioned before. Also for mode 1, Nu_{max} occurs at θ=40°, this correspond to the stagnation point. Figure 15 also shows that for mode 2, two peaks of Nu_θ exists, one on the outer surface and the other on the inner surface of the cylinder. It is seen that the values of Nu_θ for the two modes are greater than these for single cylinder.

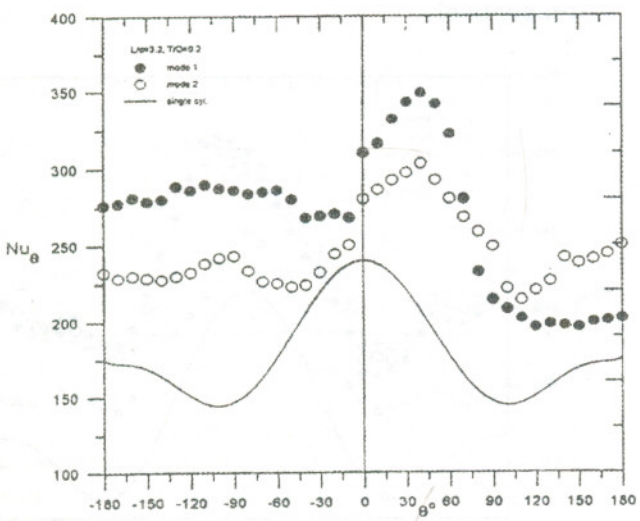

Figure 15 Distribution of local Nusselt number on the downstream cylinder at L/D =3.2 and T/D = 0.2 (Re=5.8x10⁴)

Figure 16 shows perimetric distribution of the local Nusselt number on the downstream cylinder at L/D=2.1 and different values of T/D for Re=5.8 x 10^4. It is seen that for T/D > 0.0, the maximum Nusselt number occurs at θ=30°. Figure 16 also shows that Nuθ for T/D > 0.0 is greater than that for T/D=0.0, and for isolated cylinder. At T/D=0.5, Nu_θ at 45° ≤θ≤-45° is lower than that for T/D=0.75 and 1.0. This may be attributed to the flow seperated from the upstream cylinder impinge the downstrem cylinder at θ=30° (point of maximum Nusselt number). Figure 16 also shows that At T/D=0.0, there are two peaks for Nusselt number corresponding to the two reattachment points of the separated shear layers from the upstream cylinder on the downstream cylinder.

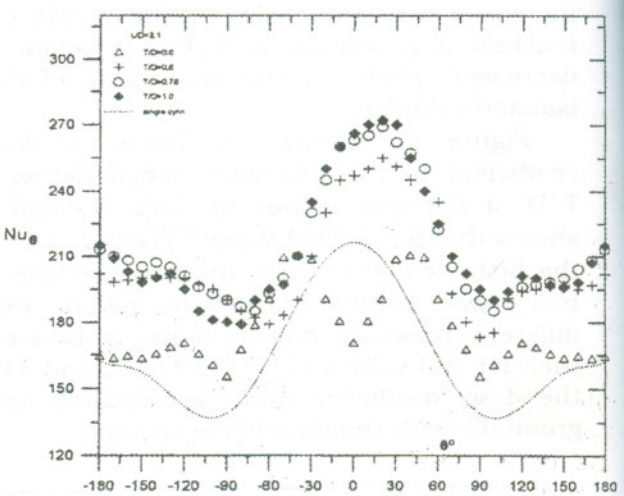

Figure 16 Perimetic distribution of the local Nusselt number on the downstream cylinder at L/D =2.1 and different values of T/D

Figures 14, 15 and 16 show that Nu_{max} on the outer surface of the downstream cylinder plays an important role for the average Nusselt number Nu_m. Therefore it is important to know the variation of Nu_{max} with L/D and T/D. Figure 17 illustrates the variation of Nu_{max} with T/D at different values of L/D. It is seen from the figure that, Nu_{max} increases with increasing value of T/D. Nu_{max} reaches a peak in the neighborhood of T/D=1.0 before it decreases back to the isolated cylinder value.

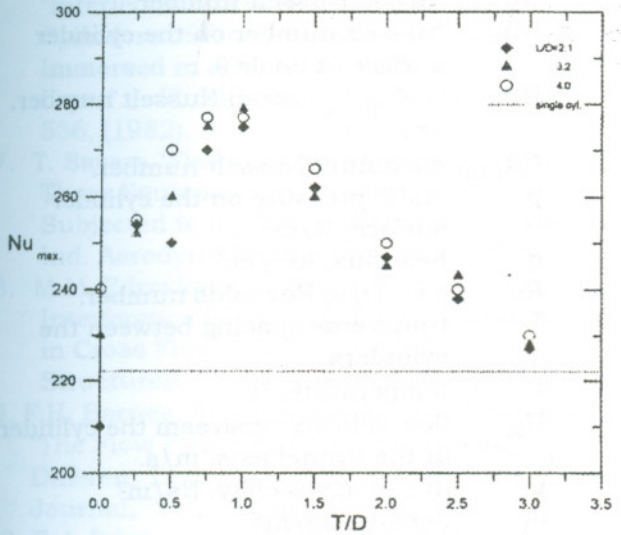

Figure 17 Variation of maximum Nusselt number with T/D at different values of L/D

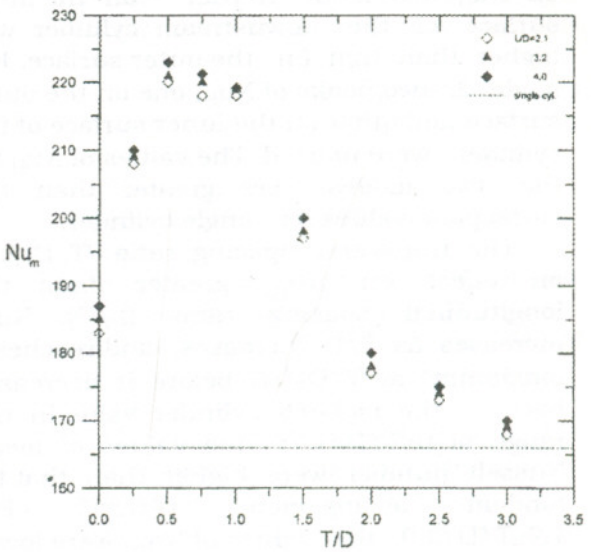

Figure 18 Variation of mean Nusselt number with T/D at different values of L/D

Mean Heat Transfer Characteristics

Figure 18 shows the variation of the mean Nusselt number with T/D at different values of L/D. It is seen that the mean Nusselt number increases with increasing value of T/D. Nu_m reaches a maximum at T/D=0.6 before it decreases back to the isolated cylinder value with further increase in T/D. In the range of $0<T/D<1.75$, the values of mean Nusselt number are higher than that for tandem arrangement (T/D=0). For $1.9\leq T/D\leq 3.0$, the values of Nu_m are lower than that for tandem arrangement (T/D=0.0). This may be attributed to the fact that interference effect in this range ($1.9\leq T/D\leq 3.0$) is lower than that for tandem arrangement. Figure 18 also shows that in the range ($0\leq T/D\leq 3$) Nu_m is higher than that for single cylinder. It is also seen that, at values of L/D=2.1,3.2, and 4, L/D has a small effect on Nu_m. Results presented in Figure 18 can be correlated as follows:

$Nu_m=196.2\ (T/D)^{0.1}\ (L/D)^{0.13}$ for
$0<T/D\leq 0.7$, and $2.1\leq L/D\leq 4.0$

$Nu_m=180\ (T/D)^{-0.2}\ (L/D)^{0.13}$
for $0.7<T/D\leq 3$, and $2.1\leq L/D\leq 4.0$
with a spread of ±5%

CONCLUSIONS

Fluid flow and heat transfer around two circular cylinders in staggered arrangement have been investigated at $Re=5.8\times 10^4$. The measurements reveal two different regimes for the lift force. In one regime, the lift force is directed toward the wake of the upstream cylinder and is due to the entrainment of the flow into the fully developed wake of the upstream cylinder. The lift force in this regime reaches a maximum value when the downstream cylinder is near to the upstream wake boundary (T/D=1.0). In the second regime, at very small spacings (T/D=0.2), the lift force becomes very large due to an intense gap flow which displaces the wake of the upstream cylinder. A discontinuity in the lift force for the staggered arrangement at (L/d)=3.2, and (T/D)=0.2 is found and is attributed to the bistable nature of the gap flow at these values of L/D and T/D.

The two bistable flow modes were observed during both pressure and temperature measurements at L/D=3.2, and T/D=0.2. However, it was noticed that the durations of the bistable values of temperature is smaller than the corresponding durations of the bistable

values of pressure. The change in the flow pattern from mode 1 to mode 2 has an effect on Nu_θ .For mode 1, Nu_θ on the inner surface of the downstream cylinder was higher than that on the outer surface. For mode 2, two peaks of Nu_θ, one on the outer surface and other on the inner surface of the cylinder were noticed. The values of Nu_θ for the two modes were greater than the correspond values for single cylinder.

The transverse spacing ratio (T/D) has an effect on Nu_m greater than the longitudinal spacing ratio (L/D). Nu_m increases as T/D increases, and reaches a maximum at $T/D \cong 0.6$ before it decreases back to the isolated cylinder value.In the range of $0<T/D<1.75$, the values of mean Nusselt number were higher than that for tandem arrangement (T/D=0). For $1.9 \le T/D \le 3.0$, the values of Nu_m were lower than that for tandem arrangement (T/D=0.0). In the range of $0 \le T/D \le 3.0$, the values of Nu_m of the downstream cylinder are higher than that for a single cylinder. A correlation of the Nu_m yielded the expressions:

$Nu_m = 196.2\ (T/D)^{0.1}\ (L/D)^{0.13}$ for $0<T/D\le 0.7$, and $2.1 \le L/D \le 4.0$

$Nu_m = 180\ (T/D)^{-0.2}\ (L/D)^{0.13}$ for $0.7<T/D\le 3$, and $2.1 \le L/D \le 4.0$

with a spread of ±5%

NOMENCLATURE

C_D $\int_0^{2\pi} \frac{1}{2} C_p \cos\theta d\theta$, drag coefficient of the cylinder.

C_L $\int_0^{2\pi} \frac{1}{2} C_p \sin\theta d\theta$,, lift coefficient of the cylinder.

C_p $\frac{p - p_\infty}{1/2 \rho U_\infty^2}$, static pressure coefficient.

D cylinder diameter, m

h $(q_w/(t_w - t\infty))$ heat transfer coefficient, $kW/m^2.K$

k thermal conductivity, kW/m.K

L longitudinal spacing between cylinders centers (in the streamwise direction).

Nu hD/k, Nusselt number.

Nu_θ Nusselt number on the cylinder surface at angle θ

Nu_m $\frac{1}{2\pi} \int_0^{2\pi} Nu_\theta d\theta$, mean Nusselt number.

Nu_{max} maximum Nusselt number.

p static pressure on the cylinder surface, N/m^2

q heat flux, kW/m^2

Re $\rho U_\infty D/\mu$, Reynolds number.

T transverse spacing between the cylinders

t temperature, °C

U_∞ flow velocity upstream the cylinders at the tunnel axis, m/s.

μ dynamic viscosity, Ns/m^2

ρ density, kg/m^3

θ central angle measured from the free stream direction (tunnel axis).

Subscripts

m mean.

max maximum.

w value at the wall.

∞ undisturbed uniform stream.

REFERENCES

1. M.M. Zdravkovich, "Review of Flow Interference between Two Circular Cylinders in Various Arrangements" J. Fluid Eng., Dec. pp. 618-633, (1977).
2. M.M. Zdravkovich, and D. L. Pridden "Interference between Two Circular Cylinders; Series of Unexpected Discontinuities" J. Ind. Aerodyn., Vol. 2, pp. 255-270, (1977).
3. A. Okajima, "Flow Around Two Tandem Circular Cylinders at Very High Reynolds Number" Bull. Jpn. Soc. Mech. Eng., Vol. 22, No. 122, pp. 504-511, (1977).
4. M. Kiya, M. Arie, H. Tamura and H. Mori, "Vortex Shedding from Two Circular Cylinders in Staggered Arrangement" J. Fluids Eng., Vol.102, pp. 166-173, (1980).
5. M.M. Zdravkovich, "Aerodynamecs of Two Parallel Circular Cylinders of Finite Height at Simulated High Reynolds Number" J. Wind Eng. Ind. Aerodyn., Vol. 6, pp. 59-71(1980).

6. S. Taniguchi, H. Sakamoto and M. Aris, "Interference between Two Circular Cylinders of Finite Length Vertically Immersed in a Turbulent Boundary Layer" J. Fluid Eng., Vol. 104, pp. 529-536, (1982).
7. T. Sayers "Flow Interference between Three Equispaced Cylinders when Subjected to a Cross Flow" J. Wind Eng. Ind. Aerodyn., Vol. 26, pp. 1-19, (1987).
8. M.M. Zdravkovich, "The Effects of Interference between Circular Cylinders in Cross Flow" J. of Fliuds and Structures, Vol. 2, pp. 239-261, (1987).
9. F.H. Barnes, A. J. Baxendale and I. Grant, "The Flow Past Two Cylinders Having Different Diameters" The Aeronatical Journal, Vol. 89, pp.125-134, (1985).
10. S.J. Price and M.P. Paidoussis "The Aerodynamic Forces Acting on Groups of Two and Three Circular Cylinders when Subjected to a Cross Flow", Journal of Wind Eng. and Industrial Aerodynamics, Vol. 17, pp. 329-347, (1984).
11. R.M. El-Taher, S.A. Sayed, and A.M.E. Abde-Latif, "The Interference Effect of a Wall on the Flow Around two Circular Cylinders", Alexandria Engineering Journal, Vol. 31, No. 4, pp. A463-473, (1992).
12. H. Osaka, I. Nakamura, H. Yamada, Y. Kuwata, and Y. Kageyama, "The Structure of a Turbulent Wake Behind a Cruciform Circular Cylinders, 1st Report: The Mean Velocity Field" Bulletin of JSME, Vol. 26, pp. 356-363, (1983).
13. H. Osaka, I. Nakamura, H. Yamada, Y. Kuwata, and Y. Kageyama, "The Structure of a Turbulent Wake Behind a Cruciform Circular Cylinders, 2nd Report: The Stream-Wise Development of Turbulent Flow Fields" Bulletin of JSME, Vol. 26, pp. 521-528, (1983).
14. M.M. Zdravkovich, "Flow Around two Intersecting Circular Cylinders" ASME Journal of Fuids Eng., Vol. 107, pp. 507-511, (1985).
15. M.M. Zdravkovich, "The Interference between Circular Cylinders Forming a Cross" J. of Fluid Mechanics, Vol. 128, pp. 231-246, (1983).
16. Y. Tomita, S. Inagaki, S. Suzuki, and H. Muramatsu, "A Coustic Characteristics of two Circular Cylinders Forming a Cross in Uniform Flow", JSME International Journal, Vol. 30, pp. 1069-1079, (1987).
17. T.A. Fox, "Wake Characteristics of Two Circular Cylinders Arranged Perpendicular to Each Other", ASME Journal of Fluids Eng., Vol. 113, pp. 45-50, (1991).
18. R.M. El-Taher "A Numerical Study of the Interference Effects in Uniform Shear Flow Over Two Circular cylinders" J. Eng. sci., Vol. 8, pp. 85-92, (1982).
19. R.M. El-Taher, "Experimental Study on the Interference between a Pair of Circular Cylinders Normal to a Uniform Shear Flow" J. Wind Eng. Ind. Aerodyn., Vol. 17, pp. 117-132, (1984).
20. R.M. EL-Taher, "Flow Around Two Parallel Circular Cylinders in a Linear Shear Flow" Journal of Wind Engineering and Industrial Aerodynamic, Vol. 21, pp. 251-272, (1985).
21. Z.G. Kostic, and S. N. Oka, "Fluid Flow and Heat Transfer with Two Cylinders in Cross Flow" Int. J. heat Mass Transfer, Vol. 15, pp. 279-299, (1972).
22. S. Aiba, "Heat Transfer Around a Tube in In-Line Tube Banks Near a Plane Wall" J. of Heat Transfer, Vol. 112, pp. 933-938 (1990).
23. S.A. Sayed, "An Experimental Investigation of Heat Transfer Around a Pair of Circular Cylinders Normal to Stream" Engineering Research Bulletin, University of Helwan, Fac. of Eng. and Tecil., Vol. 1, pp. 36-56. (1994).

Received January 9,1999
Accepted June 2, 1999

دراسة عملية لسريان المائع وأنتقال الحرارة حول زوج من الأسطوانات دائرية المقطع وفى ترتيب مائل

أحمد محمد السيد عبد اللطيف ، رفعت محمد الطاهر و إبراهيم على جاد
قسم هندسة القوى الميكانيكية - جامعة الزقازيق

ملخص البحث

تم اجراء هذا البحث العملى لدراسة سريان المائع وانتقال الحرارة حول اسطوانتيت دائريتين ومعرضين لسريان حر منتظم وفى ترتيب مائل. فى هذه الدراسة كانت المسافة الطولية (ل) تتغير فى نطاق ١-٥ق _حيث ل هى المسافة بين مركز الاسطوانتين، ق هو قطر الاسطوانة. كذلك كانت المسافة المستعرضة (ت) تتغير فى نطاق صفر - ٣ق _حيث ت هى المسافة المستعرضة بين مركز الأسطوانتين). وقد تم تحديد توزيعات الضغط الاستاتيكى ورقم ناسلت المحلى على سطح الأسطوانة الموجودة فى أتجاه مجرى السريان. وقد شاهدنا خلال قياسات الضغط ودرجات الحرارة سريانين غير مستقرين عند ل/ق = ٣,٢، ت/ق=٠,٢ . كذلك تم مناقسة رقم ناسلت المتوسط فى علاقة مع ل/ق،ت/ق. وكذلك تم الحصول على علاقات تربط بين رقم ناسلت المتوسط، ل/ق،ت/ق.